



# Topological effects of the superconducting vortex state in a TaSe<sub>3</sub> ring crystal: Observation of magnetic torque oscillations

Genki Kumagai,<sup>1</sup> Toru Matsuura,<sup>1</sup> Koichi Ichimura,<sup>1,2</sup> Kazuhiko Yamaya,<sup>2</sup> Katsuhiko Inagaki,<sup>1,2</sup> and Satoshi Tanda<sup>1,2</sup>

<sup>1</sup>*Department of Applied Physics, Hokkaido University, Kita 13, Nishi 8 Kita-ku, Sapporo 060-8628, Japan*

<sup>2</sup>*Center of Education and Research for Topological Science and Technology, Kita 13, Nishi 8 Kita-ku, Sapporo 060-8628, Japan*

(Received 21 January 2010; revised manuscript received 9 April 2010; published 11 May 2010)

We measured the magnetic torque of the ring-shaped crystals of TaSe<sub>3</sub> by using piezoresistive cantilevers to investigate the superconducting topological properties. We measured three ring samples and we observed that the magnetic torque of the ring crystals oscillates with increasing external magnetic field. The magnetic periods of Sample A (radius: 37.9 μm), Sample B (24.5 μm), and Sample C (15.6 μm) were  $2.16 \pm 6.6 \times 10^{-2}$  G,  $4.69 \pm 1.8 \times 10^{-1}$  G, and  $5.44 \pm 3.8 \times 10^{-1}$  G, respectively. We found that hundreds of vortices collectively and simultaneously penetrated the ring crystal. When such a phenomenon occurs, it is natural that the vortices in the ring crystal would be positioned along the circumference. From these results, we suggest that vortices exist as cylinder vortices in the rings, and this phenomenon provides unambiguous experimental evidence of the topological effect in a superconductor.

DOI: [10.1103/PhysRevB.81.184506](https://doi.org/10.1103/PhysRevB.81.184506)

PACS number(s): 74.25.Wx, 74.62.Bf

## I. INTRODUCTION

Topology and geometry can have various effects on physical properties. For example, when a type II superconductor is in the mixed state and the system size is small, the penetration and arrangement of vortices are influenced by the geometrical effect of the shape of the superconductors.<sup>1</sup> The system topology is also expected to affect the superconducting properties. For example, in nonorientable systems such as a Möbius strip crystal,<sup>2</sup> the possibility of an unusual vortex state has been predicted.<sup>3</sup> We should treat the system topology as one of the important parameters for investigating superconducting properties.

In this research, we measured the magnetic torque of the ring-shaped crystals of TaSe<sub>3</sub> to investigate the effects of topology on superconducting properties. The ring-shaped crystals of the quasi-one-dimensional superconductor TaSe<sub>3</sub> ( $T_c=2.0$  K) (Ref. 4) are suitable for use in investigating these topological effects because ring crystals are expected to have a topological effect on its chain-loop structure.<sup>5-11</sup> In addition, measurements performed without an electrode are appropriate for investigating these effects because this method conserves the system topology. Therefore, we employed magnetic torque measurements with microcantilevers as a method without an electrode.<sup>12</sup> We found that the magnetic torque of the ring crystals oscillates periodically below the transition temperature. We suggest that a cylinder vortex is formed in the rings as a result of the topological effects of the superconductive ring-shaped crystals.

## II. EXPERIMENTAL

We measured the magnetic torque of the ring-shaped crystals of TaSe<sub>3</sub> ( $T_c=2.0$  K) (Ref. 4) to investigate the effects of topology on superconducting properties. The TaSe<sub>3</sub> ring crystals were synthesized by the chemical-vapor transportation method.<sup>2,4</sup> The starting material was a mixture of Ta and Se with about 5% excess Se as a transport agent. Ta and quartz ampoules were baked at around 900 °C. After baking,

the mixture was sealed in a quartz ampoule and air was evacuated from the ampoule to the order of  $10^{-6}$  Torr. Next, the ampoule was placed in a furnace. The temperature of the starting material at the end of the ampoule was increased to the reaction temperature, typically 700 °C. The mixture was then kept at this temperature for a few hours. By using this method, thousands of ring crystals were synthesized per ampoule. The *b* axis is parallel to the circumferential direction and the highest conductivity is expected along this direction.

To investigate the effect of the topology we need a measurement that requires no electrode because the topology is changed by the presence of an electrode. In this study, we measured the magnetic torque by using microcantilevers.<sup>12</sup> The magnetic torque  $\tau = \mathbf{M} \times \mathbf{B}$  is produced on superconducting samples by an applied field  $\mathbf{B}$  and sample magnetization  $\mathbf{M}$ . In a homogeneous applied field, the transverse component of the sample magnetization will cause a deflection of the cantilever  $\Delta z$ , which is proportional to the magnetic torque  $\tau$ . The sample is mounted at the extremity of the lever as shown in Fig. 1.  $\Delta z$  is measured here as the change in the piezoresistance  $\Delta R$ . To detect a small change in the resistance, we used a Wheatstone bridge circuit measured with a lock-in amplifier. We compared the magnetic torque at temperatures below and above  $T_c$  to confirm the effect of the superconducting properties. The cantilever and the sample were cooled with a <sup>3</sup>He cryostat. All the measurements were performed in a magnetic shield room.

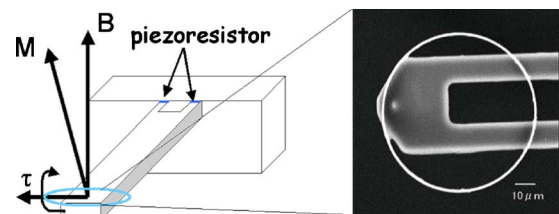


FIG. 1. (Color online) Schematic image of cantilever and ring crystal. Inset: scanning electron microscope image of TaSe<sub>3</sub> ring crystal (Sample A) and cantilever.

TABLE I. Characteristic values of the ring crystals.

| Sample name | Inner area<br>( $\mu\text{m}^2$ ) | Effective<br>inner area (45°)<br>( $\mu\text{m}^2$ ) | Radius                     |                            | Circumference<br>( $\mu\text{m}$ ) | Effective<br>circumference (45°)<br>( $\mu\text{m}$ ) | Width<br>( $\mu\text{m}$ ) |
|-------------|-----------------------------------|--|----------------------------|----------------------------|------------------------------------|---|----------------------------|
|             |                                   |  | Outer<br>( $\mu\text{m}$ ) | Inner<br>( $\mu\text{m}$ ) |                                    |   |                            |
| Sample A    | 4162                              |  | 37.9                       | 36.4                       | 228.7                              |   | 1.5                        |
| Sample B    | 897                               | 634  | 24.5                       | 16.9                       | 106.2                              | 91.2  | 7.6                        |
| Sample C    | 599                               | 424  | 15.6                       | 13.8                       | 86.9                               | 73.7  | 1.8                        |

We measured three Samples A, B, and C. The sample dimensions are summarized in Table I. With Sample A, the angle between the applied field and the ring crystal surface was  $90^\circ$ . This sample was directly measured in liquid  $^3\text{He}$ . With Samples B and C, the angle between the applied field and the ring crystal surface was  $45^\circ$ . This sample was measured in a vacuum. No difference was found between the measurement in  $^3\text{He}$  and that in a vacuum. This shows that the thermal conduction of the sample to the cold head is sufficiently high. Moreover, since this is not a dynamical method we need not worry about the damping factor. First, we swept the field in the increasing direction from 0 G. Then we swept the field in the decreasing direction. The field sweep speeds of Samples A, B, and C were  $4.4 \times 10^{-2}$  G/s,  $4.3 \times 10^{-2}$  G/s, and  $1.1 \times 10^{-2}$  G/s, respectively. In addition, we performed measurements at different rates for Samples A and C of  $4.4 \times 10^{-1}$  G/s and  $3.3 \times 10^{-3}$  G/s, respectively. With both Samples A and C, we observed the same results for measurements at different speeds. Therefore, we concluded that the speed of the field sweep has no influence on the results.

### III. RESULTS

Figures 2(a) and 2(b) are the typical results for Samples A

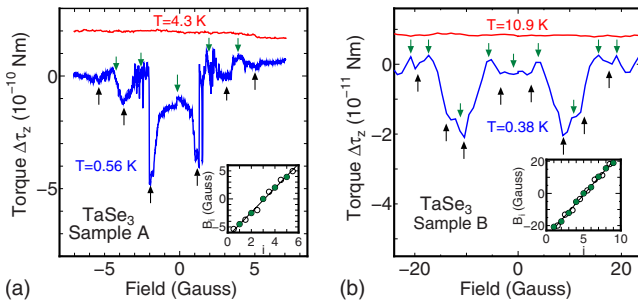


FIG. 2. (Color online) (a) Magnetic torque of Sample A as a function of the applied magnetic field. Arrows show the peak and valley positions. The blue line represents the magnetic torque measured at  $T=0.56$  K. The red line represents the torque measured at  $T=4.3$  K. Inset: open and filled circles show the valley and peak positions, respectively. (b) Magnetic torque of Sample B. Arrows show the peak and valley positions. The blue line represents the torque measured at  $T=0.38$  K. The red line represents the torque measured at  $T=10.9$  K. Inset: open and filled circles show the valley and peak positions, respectively. The magnetic torques below  $T_c=2.0$  K of both samples oscillate.

and B, respectively. For each sample, we obtained the same result for several measurements when the experimental conditions were the same. The horizontal axis shows the applied magnetic field and the vertical axis shows the magnetic torques translated from measured voltages. Offset voltages, which may be caused by residual magnetic fields, were carefully removed. Below  $T_c$ , the magnetic torques in all of the samples oscillated as a function of the applied magnetic field. These oscillations were not observed in the normal state as shown by the red line in Fig. 2. This shows that the observed oscillations originated from the superconducting state.

To demonstrate the periodicity of the oscillations, we plot their peak and valley positions as indicated by the arrows. We identify each field with indices. We plot the magnetic field of the peak and valley positions  $B_i$  as a function of index  $i$ . We found that  $B_i$  is linear to  $i$  [inset of Figs. 2(a), 2(b), and 3(a)]. The periods of Samples A, B, and C were  $2.16 \pm 6.6 \times 10^{-2}$  G,  $4.69 \pm 1.8 \times 10^{-1}$  G, and  $5.44 \pm 3.8 \times 10^{-1}$  G, respectively.

To confirm the topological effect, we performed a control experiment on a cut Sample C', after measuring Sample C. Sample C' was obtained by cutting Sample C with a focused ion beam.<sup>13,14</sup> Sample cutting is an effective method for changing the topology. Figures 3(a) and 3(b) show the typical results of these measurements. In Sample C, the magnetic torque oscillated in the same way as in Samples A and B. In Sample C', the magnetic oscillation did not appear but a broad antisymmetric peak was observed. In Sample C', when the applied magnetic field is removed, vortices may be trapped by a pinning effect at the edge. Therefore, the magnetic torque reverses when the applied magnetic field re-

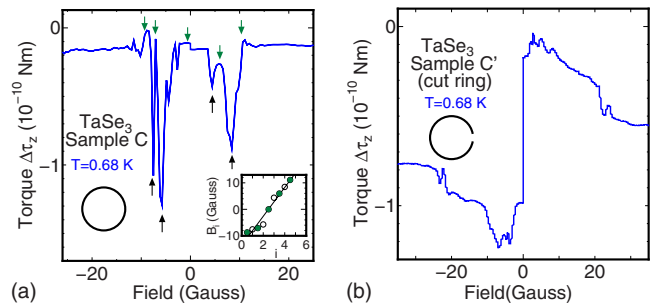


FIG. 3. (Color online) (a) Magnetic torque of Sample C at  $T=0.68$  K as a function of the applied magnetic field. Arrows show the peak and valley positions. Inset: open and filled circles show the valley and peak positions, respectively. (b) Magnetic torque of the cut Sample C' at  $T=0.68$  K.

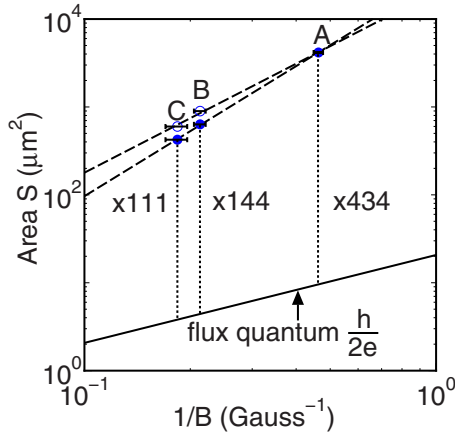


FIG. 4. (Color online) The ring area as a function of  $1/B$ .  $B$  is the period of the magnetic torque peaks. Open circles show the ring area. Filled circles show the effective ring area for  $45^\circ$ . The solid line represents  $S = \phi_0/B$ . The broken line is a guide to the eye.

verses. This is in contrast to the case with Sample C, where the direction of the magnetic torque remains unchanged when the applied magnetic field is reversed. The difference between Samples C and C' suggests that vortex state is changed by the effect of ring topology.

IV. DISCUSSION

Here we discuss the magnetic torque oscillation (Figs. 2 and 3). We assume that vortices penetrate at each period of magnetic field  $B$ . We plot the inner area  $S$  and the effective inner area (for  $45^\circ$ )  $S'$  as a function of  $1/B$  in Fig. 4. The solid line represents  $S = \phi_0/B$ , that is, the field corresponds to a flux quantum  $\phi_0 = h/2e$  per inner area. As shown in Fig. 4, we found a significant discrepancy between the solid line and the data. We estimate the number of vortices for  $90^\circ$  from  $N = BS/\phi_0$  and the number of vortices for  $45^\circ$  from  $N' = BS'/\phi_0$ :  $N = 434, 203$ , and  $157$  for Samples A, B, and C, respectively, and  $N' = 144$  and  $111$  for Samples B and C, respectively.  $N$  for Samples A and  $N'$  for Samples B and C suggest that hundreds of the vortices penetrated the samples collectively and simultaneously. This is an unprecedented phenomenon that is in contrast to the known topological effects accompanied by flux quantization.<sup>15,16</sup>

We propose a cylinder vortex model to explain the oscillation of the magnetic torque. We mean that the cylinder vortex is a cylinder formed by connecting penetrated vortices. While the magnetic field applied to the ring crystal is small, vortices cannot penetrate the ring crystal to realize the Meissner effect. Then, when the applied field increases as the vortices fill the inner area of the ring crystal, the vortices penetrate the ring crystal because of the effect of the ring-shaped topology. On the basis of the above discussion, since a number of vortices penetrate the ring crystal, we expect them to penetrate the entire ring crystal collectively and position themselves along a circumferential line rather than as

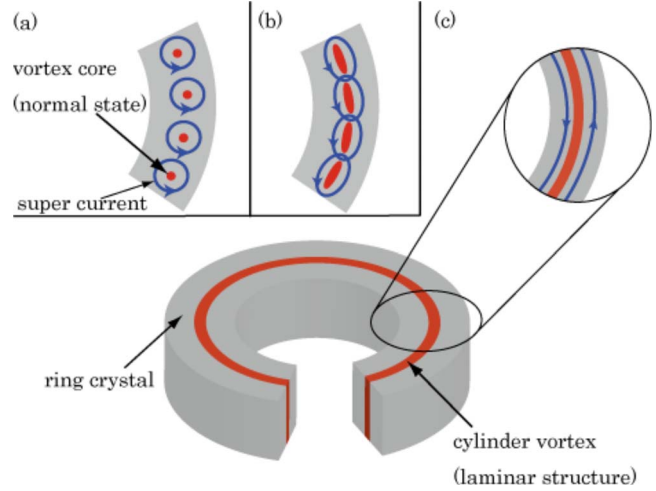


FIG. 5. (Color online) Schematic model of cylinder vortex. (a) Vortices positioned in line. (b) Vortices extending along the circle direction. (c) Vortices connected with each other and forming a cylinder vortex.

an Abrikosov lattice [Fig. 5(a)]. Moreover, vortices extend along the tangential direction owing to the strong anisotropy of the crystal structure of TaSe<sub>3</sub>.<sup>17</sup> And, the ring crystals have a  $b$  axis connecting structure. Therefore, extended vortices are stable in ring crystals and the supercurrents flowing around the vortices overlap each other [Fig. 5(b)]. This property probably causes the state whereby the vortices positioned in line connect with each other. Hence, it is natural that vortices in the ring crystal form a cylinder vortex [Fig. 5(c)]. This laminar structure was anticipated by de Gennes.<sup>18</sup> Furthermore, the length of each ring circumference divided by each  $N$  and  $N'$  is on the order of  $10^{-1} \mu\text{m}$ . This length is of the same order as the coherence length  $\xi$  of a typical superconductor. The cylinder vortex model is consistent with the fact that the magnetic torque oscillates.

V. SUMMARY

In this research, we measured magnetic torque by using piezoelectric microcantilevers. As a result, we found that the magnetic torque oscillates as the applied magnetic field increases in ring crystals and hundreds of the vortices collectively and simultaneously penetrate the ring crystal. These results indicate that vortices penetrate ring crystals as a cylinder vortex. The cylinder vortex forms as a result of the closed ring topology of the ring crystals of TaSe<sub>3</sub>.

ACKNOWLEDGMENTS

We are grateful to N. Matsunaga, K. Nomura, E. Ohmichi, Y. Nogami, and S. Takayanagi, for experimental support and discussions. This work was partially supported by the 21st century COE program on ‘‘Topological Science and Technology’’ from the Ministry of Education, Culture, Sports, Science and Technology of Japan.

- <sup>1</sup>L. F. Chibotaru, A. Ceulemans, V. Bruyndoncx, and V. V. Moshchalkov, *Phys. Rev. Lett.* **86**, 1323 (2001).
- <sup>2</sup>S. Tanda, T. Tsuneta, Y. Okajima, K. Inagaki, K. Yamaya, and N. Hatakenaka, *Nature (London)* **417**, 397 (2002).
- <sup>3</sup>M. Hayashi, H. Ebisawa, and K. Kuboki, *Phys. Rev. B* **72**, 024505 (2005).
- <sup>4</sup>S. Tanda, H. Kawamoto, M. Shiobara, Y. Okajima, and K. Yamaya, *J. Phys. IV* **9**, 379 (1999).
- <sup>5</sup>Y. Okajima, H. Kawamoto, M. Shiobara, K. Matsuda, S. Tanda and K. Yamaya, *Physica B* **284-288**, 1659 (2000).
- <sup>6</sup>T. Tsuneta and S. Tanda, *J. Cryst. Growth* **264**, 223 (2004).
- <sup>7</sup>K. Shimatake, Y. Toda, and S. Tanda, *Phys. Rev. B* **73**, 153403 (2006).
- <sup>8</sup>M. Hayashi, H. Ebisawa, and K. Kuboki, *Europhys. Lett.* **76**, 264 (2006).
- <sup>9</sup>T. Matsuura, M. Yamanaka, N. Hatakenaka, T. Matsuyama, and S. Tanda, *J. Cryst. Growth* **297**, 157 (2006).
- <sup>10</sup>T. Matsuura, K. Inagaki, and S. Tanda, *Phys. Rev. B* **79**, 014304 (2009).
- <sup>11</sup>M. Tsubota, K. Inagaki, and S. Tanda, *Physica B* **404**, 416 (2009).
- <sup>12</sup>C. Rossel, P. Bauer, D. Zech, J. Hofer, M. Willemin, and H. Keller, *J. Appl. Phys.* **79**, 8166 (1996).
- <sup>13</sup>T. Matsuura, S. Tanda, K. Asada, Y. Sakai, T. Tsuneta, K. Inagaki, and K. Yamaya, *Physica B* **329-333**, 1550 (2003).
- <sup>14</sup>T. Matsuura, T. Tsuneta, K. Inagaki, and S. Tanda, *Phys. Rev. B* **73**, 165118 (2006).
- <sup>15</sup>W. A. Little and R. P. Parks, *Phys. Rev. Lett.* **9**, 9 (1962).
- <sup>16</sup>R. C. Jaklevic, J. Lambe, A. H. Silver, and J. E. Mercereau, *Phys. Rev. Lett.* **12**, 159 (1964).
- <sup>17</sup>M. Yamamoto, *J. Phys. Soc. Jpn.* **45**, 431 (1978).
- <sup>18</sup>P. G. de Gennes, *Superconductivity of Metals and Alloys* (Addison-Wesley, New York, 1989), pp. 71–74.